Inorg. Chem. **2002**, *41*, 1236–1244

Microwave Spectra, Geometries, and Hyperfine Constants of OCAgX (X = F, Cl, Br)

Nicholas R. Walker and Michael C. L. Gerry*

Department of Chemistry, The University of British Columbia, 2036 Main Mall, Vancouver, British Columbia, Canada V6T 1Z1

Received September 25, 2001

A pulsed jet cavity Fourier transform microwave spectrometer has been used to measure the rotational spectra of OCAgX (X = F, Cl, Br) in the frequency range 5–22 GHz. Metal atoms were generated via laser ablation and were allowed to react with CO and a halide precursor, prior to stabilization of the products within a supersonic jet of argon. These are the first experimental observations of OCAgF and OCAgBr, and the first high resolution spectroscopic study of OCAgCl. All three molecules are linear. Accurately determined rotational constants have been used to evaluate the various internuclear distances, which are found to be consistent with trends established for OCAuX and OCCuX species. The C–O distances are short, and the M–C distances are significantly longer than those in other molecules containing a metal–carbonyl bond. Precise values of centrifugal distortion constants and halogen nuclear quadrupole coupling constants have also been determined. The coupling constants are compared with the results of previous studies of OCCuX and OCAuX and are used to infer trends in the electron distributions of the molecules. Ab initio calculations have been performed and employed to predict the geometries, vibrational frequencies, and Mulliken valence orbital populations of the various species.

I. Introduction

Although transition metal carbonyls are ubiquitous, the vast majority involve the metals of groups 5−10. There are very few reported neutral carbonyl compounds of the coinage metals, Cu, Ag, and Au (group 11), particularly for Ag and Au. For Au, these are restricted to complexes containing a "weakly coordinating anion",[1] plus the carbonyl halides OCAuX (X = F, Cl, Br).[2,3,4] For Ag, the only reports[5,6] prior to 2001 were of $Ag(CO)_n^+$ (n = 1, 2).

The bonding in group 11 carbonyls appears to be unusual. For most nonbridging carbonyls, the CO stretching frequency is considerably less than that of free CO. This has led to the conventional model of metal−carbonyl bonding, which holds that the carbon atom acts as a σ-donor and that there is synergistic π-back-donation from metal d-orbitals to the antibonding π^*-orbitals on CO. The bonding in the CO moiety is thus weakened, leading to the lowering of the stretching frequency. However, the known Ag and Au carbonyls all have CO stretching frequencies greater than that of free CO.[1,6−9] This has led to the suggestion that for the noble metal carbonyls the π-back-bonding is essentially nonexistent.[6]

Prior to 2001, only three coinage metal carbonyl halides had been prepared. OCAuCl has been known for over seventy years;[2,3] it is a solid containing discrete linear molecules.[10] OCAuBr, which has been recently reported, is much less stable than the chloride.[9] The third known substance was OCCuCl. As a pure compound, it has a polymeric layer structure.[11] When isolated in a matrix, it is a linear OCCuCl monomer.[12]

The chlorides OCMCl (M = Cu, Ag, Au) have, however, attracted the attention of quantum chemists. Plitt et al.[12] used

* To whom correspondence should be addressed. E-mail: mgerry@chem.ubc.ca. Fax: (604) 822-2847.

(1) Willner, H.; Schaebs, J.; Hwang, G.; Mistry, F.; Jones, R.; Trotter, J.; Aubke, F. *J. Am. Chem. Soc*. **1992**, *114*, 8972.
(2) Karasch, M. S.; Isbell, M. S. *J. Am. Chem. Soc.* **1930**, *52*, 2919.
(3) Manchot, W.; Gall, H. *Chem. Ber*. **1925**, *58*, 2175.
(4) Evans, C. J.; Reynard, L. M.; Gerry, M. C. L. *Inorg. Chem*. **2001**, *40*, 6123.
(5) Manchot, W.; König, J. *Chem. Ber*. **1927**, *60*, 2183.
(6) Hurlburt, P. K.; Rack, J. J.; Luck, J. S.; Dec, S. F.; Webb, J. D.; Anderson, O. P.; Strauss, S. H. *J. Am. Chem. Soc.* **1994**, *116*, 10003.
(7) Dell'Amico, D.; Calderazzo, F. *Gazz. Chim. Ital*. **1973**, *103*, 1099.
(8) Browning, J.; Goggin, P. L.; Goodfellow, R. J.; Norton, M. G.; Rattray, A. J. M.; Taylor, B. F.; Mink, J. *J. Chem. Soc., Dalton Trans.* **1977**, 2061.
(9) Dell'Amico, D.; Calderazzo, F.; Robino, P.; Segre, A. *J. Chem. Soc. Dalton Trans.* **1991**, 3017.
(10) Jones, P. G. *Z. Naturforsch., B: Chem. Sci.* **1982**, *37*, 823.
(11) Hakansson, M.; Jagner, S. *Inorg. Chem*. **1990**, *29*, 5241.
(12) Plitt, H. S.; Bär, M. R.; Ahlrichs, R.; Schnöckel, H. *Inorg. Chem.* **1992**, *31*, 463.

10.1021/ic010997m CCC: $22.00 © 2002 American Chemical Society
Published on Web 02/12/2002

ab initio calculations to confirm the existence of OCCuCl. Subsequently, Antes et al.[13] carried out extensive calculations which included relativistic core potentials for the metals. They predicted geometries, stretching force constants, dissociation energies, dipole moments, and ^{35}Cl electric field gradients. They also obtained Mulliken populations predicting sizable π-back-donation from the metal to CO, which is not in keeping with the simple rationale for the high CO stretching frequency given previously; this result has been corroborated very recently.[4,14] Very recently, Shao et al.[15] used a density functional (B3LYP) calculation on OCAgCl to predict its geometry and to assign its CO stretching mode in a matrix isolation infrared study.

Recently, we have shown that it is possible to prepare complexes of general formula NgMX, where Ng = Ar, Kr; M = Cu, Ag, Au; X = F, Cl, Br. They were generated via laser ablation of the metal, stabilized in supersonic jets of noble gas, and characterized by Fourier transform microwave (FTMW) spectroscopy.[16−21] They were found to be unusually rigid, with very short noble gas−noble metal bonds. The Cu and Au nuclear quadrupole coupling constants indicated large electron reorganization when the complexes are formed from MX monomers. Ab initio calculations, including Mulliken population analyses, showed a degree of covalent bonding between the noble gas and the metal.

This work has now been extended to the corresponding OCMX complexes. Two earlier papers reported the spectra of the Au and Cu derivatives, which were very easy to prepare by this technique.[4,14] For OCAuF, OCCuF, and OCCuBr, these were the first reports of any kind. For all these molecules, the CO internuclear distances were found to be close to or slightly greater (by <0.006 Å) than that of free CO. In addition, the M−C bonds were found to be relatively long. However, ab initio calculations for all six halides again indicated significant M−CO π-back-donation ($\sim$0.2 electron).

The present paper reports the microwave spectra of OCAgX (X = F, Cl, Br). These molecules were previously thought to be difficult to prepare,[13] and for two of them, these are the first experimental observations of any kind. They were easily prepared by our technique: laser ablation of Ag in the presence of CO and a halogen precursor (SF_6, Cl_2, and Br_2) contained in the Ar backing gas of a pulsed supersonic jet. Internuclear distances and hyperfine constants have been determined for each molecule; all three molecules are linear. The results are discussed with reference to theoretical calculations and also with reference to trends found for OCCuX, OCAuX, and other complexes containing metal−carbonyl bonds.

II. Experimental Methods

The complexes were generated using a laser ablation system in conjunction with a Balle−Flygare type[22] cavity pulsed-jet Fourier transform microwave (FTMW) spectrometer. The system has been described at length in earlier papers,[23−25] so only a brief description is provided here. The microwave cavity is composed of two spherical aluminum mirrors (28 cm diameter, radius of curvature 38.4 cm) separated by approximately 30 cm. One mirror is fixed, and the other is manually adjustable to permit the cavity to be tuned to the polarization frequency. The pulsed supersonic jet of gas enters the microwave cavity via a General Valve (series 9) nozzle mounted slightly off-center in the fixed mirror. This configuration optimizes the sensitivity and resolution of the spectrometer but causes all the lines to be observed as Doppler pairs because the direction of microwave propagation is parallel to the direction of the supersonic jet. The line position is determined by finding the average frequency of the two Doppler components. All measurements are referenced to a Loran C frequency standard that is accurate to 1 part in 10^{10}.

Generation of the complexes was facilitated by the ablation of a silver rod using the second harmonic of a Nd:YAG laser. The rod was situated approximately 5 mm from the orifice of the pulsed nozzle and was continuously rotated and translated to expose a fresh surface of metal to the laser prior to each shot. A gas mixture consisting of 0.05−0.15% halogen-containing precursor, 1.5% carbon monoxide, and argon (backing pressure, $\sim$6 atm) was introduced through the pulsed nozzle. These concentrations were found to yield lines of optimal intensity. The precursors of the halogen atoms were SF_6, Cl_2, and Br_2, for F, Cl, and Br, respectively. To obtain data from a range of isotopomers, isotopically enriched ^{13}CO, $^{13}C^{18}O$, or $C^{18}O$ was employed where appropriate. The complexes were stabilized in the collision-free environment of the supersonic expansion.

Two sources of silver were employed during the experiments: (a) a rod consisting of silver in the naturally occurring distribution of isotopic abundances (Goodfellow, 99.9% pure) and (b) a rod overlaid with a thin sheet of isotopically enriched ^{107}Ag foil. The foil was produced by melting ^{107}Ag powder (Cambridge Isotopes, 99.9% pure) to produce a solid sample of ^{107}Ag and then flattening the solid to a foil using a hammer. Use of the isotopically enriched sample assisted the unambiguous assignment of the spectra of several isotopomers which had extensively overlapped transitions.

III. Quantum Chemical Calculations

The geometries of the three molecules were optimized at the second-order Møller−Plesset[26] level of theory using the GAUSSIAN 98[27] suite of programs. The vibrational wavenumbers were calculated for OCAgF and OCAgCl; Mulliken orbital populations were calculated for all three molecules. Calculations were also performed on the analogous metal halides (AgF, AgCl, and AgBr). The 6-311G**[28] basis set was used for the O, C, and F atoms. A relativistic effective core potential (RECP) was used for silver, leaving 19 valence electrons ($4s^24p^64d^{10}5s^1$). The RECP and Gaussian basis set for Ag (31111s/22111p/411d) were taken from

(13) Antes, I.; Dapprich, S.; Frenking, G.; Schwerdtfeger, P. *Inorg. Chem.* **1996**, *35*, 2089.
(14) Walker, N. R.; Gerry, M. C. L. *Inorg. Chem.* **2001**, *40*, 6158.
(15) Shao, L.; Zhang, L.; Zhou, M.; Qin, Q. *Organometallics* **2001**, *20*, 1137.
(16) Evans, C. J.; Gerry, M. C. L. *J. Chem. Phys.* **2000**, *112*, 1321.
(17) Evans, C. J.; Gerry, M. C. L. *J. Chem. Phys.* **2000**, *112*, 9363.
(18) Evans, C. J.; Lesarri, A.; Gerry, M. C. L. *J. Am. Chem. Soc.* **2000**, *122*, 6100.
(19) Evans, C. J.; Rubinoff, D. S.; Gerry M. C. L. *Phys. Chem. Chem. Phys.* **2000**, *2*, 3943.
(20) Reynard, L. M.; Evans, C. J.; Gerry M. C. L. *J. Mol. Spectrosc.* **2001**, *206*, 33.
(21) Walker, N. R.; Reynard L. M.; Gerry, M. C. L. *J. Mol. Structure*, in press.
(22) Balle, T. J.; Flygare, W. H. *Rev. Sci. Instrum.* **1981**, *52*, 33.
(23) Xu, Y.; Jäger, W.; Gerry M. C. L. *J. Mol. Spectrosc.* **1992**, *151*, 206.
(24) Brupbacher, T.; Bohn, R. K.; Jäger, W.; Gerry, M. C. L.; Pasinszki, T.; Westwood, N. P. C. *J. Mol. Spectrosc.* **1997**, *181*, 316.
(25) Walker K. A.; Gerry, M. C. L. *J. Mol. Spectrosc.* **1997**, *182*, 178.
(26) Møller, C.; Plesset, M. S. *Phys. Rev.* **1934**, *46*, 618.

Andrae et al.[29] The Ag basis set was augmented with two f functions ($\alpha_f = 3.1235$ and $\alpha_f = 1.3375$).[13] The (631111s/52111p) McLean−Chandler[30] basis set, augmented with a d-polarization function[13] ($\alpha_d = 0.75$), was used for Cl. The aug-cc-pVTZ basis set was used for Br.[31]

IV. Assigned Spectra and Analyses

A. Spectrum of OCAgCl. An initial estimate for the rotational constant of $^{16}O^{12}C^{107}Ag^{35}Cl$ was made using the equilibrium structure calculated by Antes et al.[13] After an extensive search, several lines were identified near 10530 MHz, approximately 250 MHz lower than the position predicted for $J = 4-3$ of the described species. The lines were observed readily, requiring only 5 averaging cycles to be distinguished from the background noise. Four lines were found, however, instead of the predicted two; they are depicted in Figure 1a. By analogy with ArAgCl, the second pair was assigned to a second isotopomer, $^{16}O^{12}C^{109}Ag^{35}Cl$. The rotational constant B_0 was revised using the measured positions of these lines, and its new value was then used to locate several further transitions. They confirmed that the molecule is linear. A preliminary structure which assumed that the C−O and Ag−Cl bond lengths were unchanged on complex formation was used to predict the rotational constants of the two ^{37}Cl-containing species, $^{16}O^{12}CAg^{37}Cl$. Their spectra were readily assigned.

The close proximity of the lines of pairs of isotopomers containing ^{107}Ag and ^{109}Ag indicates that the silver atom is very close to the molecular center of mass. The lines are so close that the assignment to a given isotopomer could not be based simply on the rigid rotor. Zero-point vibrational effects can cause the higher mass isotopomer to have the higher rotational constant.[32] Yet even where the rotational constant differences are very small, it is essential to make the correct isotopic assignments to obtain reliable structural parameters. This is especially the case when the structural method used (see later) attempts to account for the vibrational effects. A similar concern arose also for OCCuCl,[14] where Cu is also close to the molecular center of mass, and there

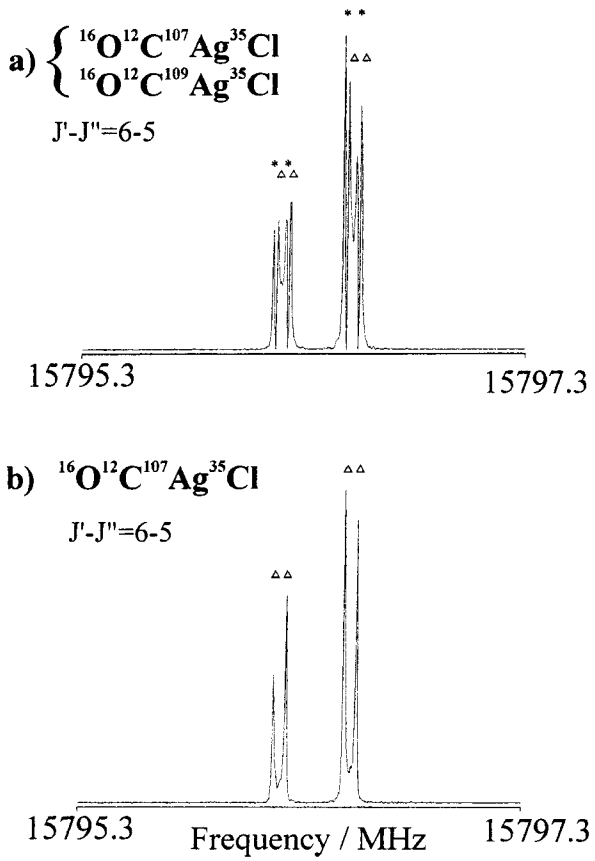

Figure 1. (a) Hyperfine structure in the $J'-J'' = 6-5$ transitions of $^{16}O^{12}C^{107}Ag^{35}Cl$ and $^{16}O^{12}C^{109}Ag^{35}Cl$. Experimental conditions: 0.2 μs microwave pulse width, 70 averaging cycles, 4k data points, 4k transform. The lines were measured using a silver rod containing the naturally occurring distribution of isotopic abundances. There are four lines present; those indicated with a triangle are assigned to the ^{107}Ag isotopomer, and an asterisk indicates those lines assigned to the spectrum of the ^{109}Ag-containing isotopomer. In each case, the higher frequency line is assigned to both $F'-F'' = 15/2-13/2$ and $11/2-9/2$, while the lower frequency line is assigned to both $F'-F'' = 9/2-7/2$ and $11/2-9/2$. (b) Hyperfine structure in the $J'-J'' = 6-5$ transition of $^{16}O^{12}C^{107}Ag^{35}Cl$. Experimental conditions: 0.2 μs microwave pulse width, 100 averaging cycles, 4k data points, 4k transform. The lines were measured using a sample of isotopically enriched ^{107}Ag. Therefore, only the transitions (described previously) assigned to the ^{107}Ag-containing species are present.

are two abundant Cu isotopes (^{63}Cu and ^{65}Cu) which produce heavily overlapped spectra. In that case, correct assignments were made readily because the two Cu isotopes have different quadrupole moments and produce different hyperfine splittings. It helped also that the two Cu isotopes have different abundances.

For OCAgCl, where the two Ag isotopes have zero nuclear quadrupole moment and nearly equal abundances, correct isotopic assignments could be made only by using the isotopically enriched ^{107}Ag mentioned previously. Figure 1 shows how this was applied. Whereas Figure 1a shows the lines observed using naturally occurring Ag, Figure 1b shows those observed using pure ^{107}Ag. The assignment was straightforward. In this case, the rigid rotor order was followed; the ^{107}Ag-isotopomer has higher frequency lines than the ^{109}Ag-containing isotopomer.

To permit accurate determination of all the internuclear distances, spectra were measured also for isotopomers containing $^{13}C^{16}O$, $^{12}C^{18}O$, and $^{13}C^{18}O$. In all, spectra of 10

(27) Frisch, M. J.; Trucks, G. W.; Schlegel, H. B.; Scuseria, G. E.; Robb, M. A.; Cheeseman, J. R.; Zakrzewski, V. G.; Montgomery, J. A., Jr.; Stratmann, R. E.; Burant, J. C.; Dapprich, S.; Millam, J. M.; Daniels, A. D.; Kudin, K. N.; Strain, M. C.; Farkas, O.; Tomasi, J.; Barone, V.; Cossi, M.; Cammi, R.; Mennucci, B.; Pomelli, C.; Adamo, C.; Clifford, S.; Ochterski, J.; Petersson, G. A.; Ayala, P. Y.; Cui, Q.; Morokuma, K.; Malick, D. K.; Rabuck, A. D.; Raghavachari, K.; Foresman, J. B.; Cioslowski, J.; Ortiz, J. V.; Stefanov, B. B.; Liu, G.; Liashenko, A.; Piskorz, P.; Komaromi, I.; Gomperts, R.; Martin, R. L.; Fox, D. J.; Keith, T.; Al-Laham, M. A.; Peng, C. Y.; Nanayakkara, A.; Gonzalez, C.; Challacombe, M.; Gill, P. M. W.; Johnson, B. G.; Chen, W.; Wong, M. W.; Andres, J. L.; Head-Gordon, M.; Replogle, E. S.; Pople, J. A. *Gaussian 98*, revision A.7; Gaussian, Inc.: Pittsburgh, PA, 1998.
(28) Krishnan, R.; Binkley, J. S.; Seeger, R.; Pople, J. A. *J. Chem. Phys.* **1980**, *72*, 650.
(29) Andrae, D.; Häusermann, V.; Dolg, M.; Støll, H.; Preus, H. *Theor. Chim. Acta* **1990**, *77*, 123.
(30) McLean, A.; Chandler, G. S. *J. Chem. Phys.* **1980**, *72*, 5639.
(31) (a) Woon, D. E.; Dunning, T. H., Jr. *J. Chem. Phys.* **1993**, *98*, 1358. (b) Wilson, A. K.; Woon, D. E.; Peterson, K. A.; Dunning, T. H., Jr. *J. Chem. Phys.* **1999**, *110*, 7667.
(32) Starck, B. Molecular Constants from Microwave Spectroscopy. *Landolt-Börnstein Numerical Data and Functional Relationships in Science and Technology*; New Series; Springer-Verlag: Berlin, 1967; Vol. II/4, p 22.

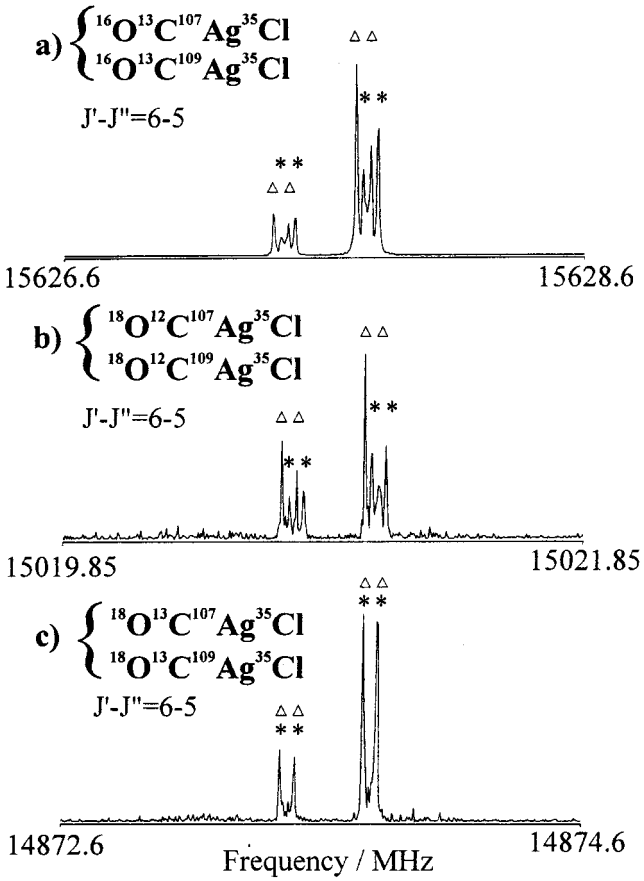

Figure 2. Lines in the J′−J″ = 6−5 transitions of (a) $^{16}O^{13}CAg^{35}Cl$ (0.2 μs microwave pulse width, 50 averaging cycles, 4k data points, 4k transform), (b) $^{18}O^{12}CAg^{35}Cl$ (0.2 μs microwave pulse width, 200 averaging cycles, 4k data points, 4k transform), and (c) $^{18}O^{13}CAg^{35}Cl$ (0.2 μs microwave pulse width, 50 averaging cycles, 4k data points, 4k transform). As in Figure 1, those lines assigned to isotopomers containing ^{107}Ag are indicated with triangles, and asterisks designate lines assigned to isotopomers containing ^{109}Ag. The quantum numbers for the transitions are the same as those provided in Figure 1. In part c, the lines arising from both ^{107}Ag- and ^{109}Ag-containing isotopomers are overlapped.

isotopomers containing ^{13}C and/or ^{18}O were measured. Because $^{13}C^{18}O$ was present only as an impurity (14.6%) in a sample of $^{13}C^{16}O$, the lines of $^{13}C^{18}O$-containing species were relatively weak. *In all cases*, the pure ^{107}Ag sample was used to assign each spectrum to the correct isotopomer. It was found that of all the observed isotopomers containing isotopically enriched CO, only the pair $^{16}O^{13}CAg^{37}Cl$ showed the rigid rotor isotopic ordering.

Figure 2 shows lines of several isotopomers containing isotopically enriched CO. Figure 2a, b shows transitions of $^{16}O^{13}CAg^{35}Cl$ and $^{18}O^{12}CAg^{35}Cl$, in which the lines of the ^{107}Ag isotopomer are ∼28 kHz *lower* in frequency than those of the ^{109}Ag isotopomer. A comparable pattern was also found for $^{18}O^{12}CAg^{37}Cl$ (not shown in the figure).

Figure 2c shows a transition of $^{18}O^{13}CAg^{35}Cl$, with Ag in its natural isotopic distribution. It contains only two lines instead of its anticipated four. Use of the enriched ^{107}Ag confirmed that the lines could be attributed, at least in part, to the ^{107}Ag-containing species. An exhaustive search did not reveal additional lines within 10 MHz, yet it is clear from the spectra of the other isotopomers that the lines of the ^{109}Ag-containing species should be no more than a few

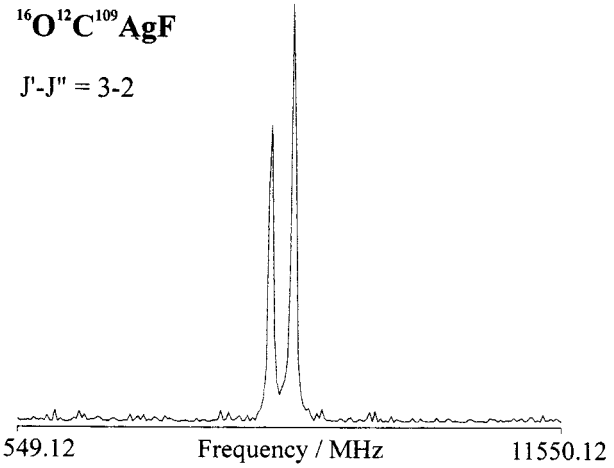

Figure 3. J′−J″ = 3−2 transition of $^{16}O^{12}C^{109}AgF$. Experimental conditions: 0.2 μs microwave pulse width, 100 averaging cycles, 4k data points, 4k transform.

tens of kilohertz away. The inevitable conclusion is that the spectra of the ^{107}Ag and ^{109}Ag species are overlapped. To test this idea, a series of structure fits was performed to determine the effect of data obtained from the $^{13}C^{18}O$-containing species on the resulting structures. The $r_m^{(2)}$ method (described later) was used, because it was expected to be the most sensitive to isotopic variations. It was found that the same $r_m^{(2)}$ internuclear distances were obtained whether or not these isotopomers were included, but that residuals in the fit were lower when they were included. The residuals also showed that the two isotopomers should have the same rotational constants. Thus, their spectra are indeed completely overlapped, to the resolution of the technique, an astonishing occurrence. The final structure fits discussed later assumed these lines were due to both isotopomers.

B. Spectra of OCAgF and OCAgBr. The results from the work of Evans et al.[16] on ArAgCl and ArAgF assisted in the prediction of the rotational constant of OCAgF. The ratio of the respective M−Ar internuclear distances in these compounds was calculated, and it was assumed that this ratio would be the same for the C−Ag internuclear distances in OCAgCl and OCAgF. The Ag−F and C−O distances were assumed to approximate those in monomeric AgF and CO, respectively. This procedure yielded a rotational constant that was found to be relatively accurate; the $J = 2-1$ transition of $^{16}O^{12}C^{107}AgF$ was detected at ∼7699 MHz, less than 40 MHz from its predicted position. Further lines were collected, and an example of the $J = 3-2$ transition of $^{16}O^{12}C^{109}AgF$ is shown in Figure 3. Again, the molecule is linear. Results were acquired from six isotopomers, permitting a precise calculation of the C−O and Ag−C distance. The spectra of the various isotopomers of ^{107}Ag and ^{109}Ag were separated by several MHz, so the isotopically enriched sample of ^{107}Ag was not needed for this molecule.

Similarly, the Ag−C distance in OCAgBr was initially estimated assuming that these distances in OCAgBr and OCAgCl were in the same ratio as the Ar−Ag distances in ArAgBr and ArAgCl. This enabled some $^{16}O^{12}C^{107}Ag^{79}Br$ transitions to be identified near ∼8520 MHz, within 50 MHz of their predicted frequencies. This molecule is also linear.

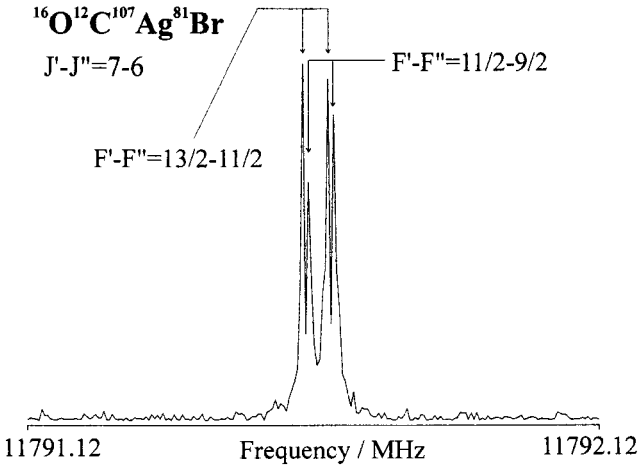

Figure 4. Hyperfine structure in the $J'-J'' = 7-6$ transition of $^{16}O^{12}C^{107}Ag^{81}Br$: 0.2 μs microwave pulse width, 100 averaging cycles, 4k data points, 4k transform.

The spectra of eleven more isotopomers permitted the accurate determination of the O−C, Ag−C, and Ag−Br distances. Again, the isotopically enriched sample of ^{107}Ag was not required. A pair of lines from the spectrum of $^{16}O^{12}C^{107}Ag^{81}Br$ is in Figure 4.

C. Analyses of the Spectra. The spectra of all isotopomers of OCAgCl and OCAgBr showed nuclear quadrupole hyperfine structure due to Cl and Br, respectively. Quantum number assignments for these molecules were made according to the coupling scheme $\mathbf{J} + \mathbf{I} = \mathbf{F}$. No hyperfine structure was observed for OCAgF, so only J assignments were required. The measured line frequencies and their assignments are given in the Supporting Information.

For each molecule, the line positions were subjected to least-squares fitting using Pickett's weighted least-squares fitting program SPFIT.[33] The data were fitted to a Hamiltonian of the form

$$\mathbf{H} = \mathbf{H}_{\text{rot}} + \mathbf{H}_{\text{nucl.quad}} \tag{1}$$

where

$$\mathbf{H}_{\text{rot}} = B_0\mathbf{J}^2 - D_J\mathbf{J}^4 \tag{2}$$

$$\mathbf{H}_{\text{nucl.quad}} = -\frac{1}{6}(\mathbf{V}_X \cdot \mathbf{Q}_X) \tag{3}$$

The fitted constants were the rotational constant (B_0), the centrifugal distortion constant (D_J), and where necessary, the halogen nuclear quadrupole coupling constant in eq 3, eQq(X). B_0 and D_J were determined for every isotopomer of each molecule studied. Values for eQq(X) were obtained for chlorine and bromine. The residuals in the fits were typically less than 1 kHz. The resulting constants are in Tables 1−3 for OCAgF, OCAgCl, and OCAgBr, respectively.

V. Structures of the Complexes

A. Structural Calculations. The possibility of precise molecular structure determination is among the principal advantages of microwave spectroscopy. Line frequencies are typically measured to an accuracy of ±1 kHz, and rotational constants can be evaluated to a correspondingly high level of precision. When sufficient isotopic data can be acquired from molecules in excited vibrational states, accurate equilibrium (r_e) distances can be calculated. Unfortunately, no lines from excited vibrational states were observed for any of the molecules studied during this work. The internuclear distances were therefore determined using several more approximate methods.

***Effective Structures* − r_0.** Calculation of a ground-state effective structure neglects the contributions made by vibrational effects to the measured ground-state rotational constants, B_0.[34] The moments of inertia I_0 are calculated directly from the experimental rotational constants using $I_0 = h/8\pi^2B_0$. These moments of inertia are assumed to be functions of the internuclear distances according to the rigid rotor expression:

$$I_0 = I_{\text{rigid}}(r_0) \tag{4}$$

In the present work, for each molecule, the three internuclear distances were fit by least squares to the experimental rotational constants of Tables 1−3. The resulting r_0 distances are presented in Table 4.

***Fitted Substitution Structures* − $r_{I\epsilon}$.** A more accurate structural determination can be obtained where the importance of vibrational effects is acknowledged. In the calculation of $r_{I\epsilon}$ structures, the magnitude of the vibrational contribution is assumed to be independent of isotopomer, and the fits are made to the internuclear distances plus an additional parameter ϵ, according to the equation[35]

$$I_0 = I_{\text{rigid}}(r_{I\epsilon}) + \epsilon \tag{5}$$

The same assumption is made in the conventional substitution (r_s) method.[36] Where data have been obtained from several isotopic species, therefore, the determined structures should be the same. The $r_{I\epsilon}$ distances determined for the various OCAgX species are shown in Table 4. Because an additional fitted parameter is employed in the calculation of

Table 1. Molecular Constants Calculated for Various Isotopomers of OCAgF in Megahertz

parameter	$^{16}O^{12}C^{107}AgF$	$^{16}O^{12}C^{109}AgF$
B_0	1925.73678(18)[a]	1924.93875(18)
$D_J \times 10^4$	2.519(47)	2.495(47)
	$^{16}O^{13}C^{107}AgF$	$^{16}O^{13}C^{109}AgF$
B_0	1904.07658(14)	1903.22036(18)
$D_J \times 10^4$	2.384(25)	2.460(47)
	$^{18}O^{12}C^{107}AgF$	$^{18}O^{12}C^{109}AgF$
B_0	1814.17037(14)	1813.22247(14)
$D_J \times 10^4$	2.237(25)	2.197(25)

[a] Numbers in parentheses are 1 SD in units of the last significant figure.

(33) Pickett, H. M. *J. Mol. Spectrosc.* **1991**, *148*, 371.
(34) Gordy, W.; Cook, R. L. Microwave Molecular Spectra. *Techniques of Chemistry, No. XVIII*, 3rd ed.; Wiley: New York, 1984.
(35) Rudolph, H. D. *Struct. Chem.* **1991**, *2*, 581.
(36) Costain, C. C. *J. Chem. Phys.* **1958**, *29*, 864.

Table 2. Molecular Constants Calculated for Various Isotopomers of OCAgCl in Megahertz

parameter	$^{16}O^{12}C^{107}Ag^{35}Cl$	$^{16}O^{12}C^{109}Ag^{35}Cl$	$^{16}O^{12}C^{107}Ag^{37}Cl$	$^{16}O^{12}C^{109}Ag^{37}Cl$
B_0	1316.376971(64)[a]	1316.375186(62)	1283.654457(99)	1283.640287(91)
$D_J \times 10^4$	1.1565(97)	1.1365(94)	1.085(14)	1.096(12)
eQq(Cl)	−28.1515(18)	−28.1505(18)	−22.0407(19)	−22.2017(19)
	$^{16}O^{13}C^{107}Ag^{35}Cl$	$^{16}O^{13}C^{109}Ag^{35}Cl$	$^{16}O^{13}C^{107}Ag^{37}Cl$	$^{16}O^{13}C^{109}Ag^{37}Cl$
B_0	1302.311820(72)	1302.314129(72)	1269.938442(79)	1269.931554(72)
$D_J \times 10^4$	1.1299(75)	1.1470(75)	1.0813(82)	1.0692(75)
eQq(Cl)	−28.158(33)	−28.140(26)	−22.206(46)	−22.180(26)
	$^{18}O^{12}C^{107}Ag^{35}Cl$	$^{18}O^{12}C^{109}Ag^{35}Cl$	$^{18}O^{12}C^{107}Ag^{37}Cl$	$^{18}O^{12}C^{109}Ag^{37}Cl$
B_0	1251.75158(11)	1251.75418(11)	1221.15872(12)	1221.16152(12)
$D_J \times 10^4$	1.016(13)	1.055(14)	0.966(14)	1.072(15)
eQq(Cl)	−28.186(20)	−28.146(20)	−22.180(38)	−21.754(60)
	$^{18}O^{13}C^{107}Ag^{35}Cl$	$^{18}O^{13}C^{109}Ag^{35}Cl$		
B_0	1239.48074(12)	1239.48074(12)		
$D_J \times 10^4$	1.015(22)	1.015(22)		
eQq(Cl)	−28.161(27)	−28.161(27)		

[a] Numbers in parentheses are 1 SD in units of the last significant figure.

Table 3. Molecular Constants Calculated for Various Isotopomers of OCAgBr in Megahertz

parameter	$^{16}O^{12}C^{107}Ag^{79}Br$	$^{16}O^{12}C^{109}Ag^{79}Br$	$^{16}O^{12}C^{107}Ag^{81}Br$	$^{16}O^{12}C^{109}Ag^{81}Br$
B_0	851.753432(45)[a]	850.971850(47)	842.187245(47)	841.372486(47)
$D_J \times 10^4$	0.4989(33)	0.4985(34)	0.4892(33)	0.4880(33)
eQq(Br)	223.902(66)	223.903(47)	187.005(45)	187.029(48)
	$^{16}O^{13}C^{107}Ag^{79}Br$	$^{16}O^{13}C^{109}Ag^{79}Br$	$^{16}O^{13}C^{107}Ag^{81}Br$	$^{16}O^{13}C^{109}Ag^{81}Br$
B_0	842.511552(62)	841.781384(58)	833.030502(58)	832.268105(58)
$D_J \times 10^4$	0.4873(53)	0.4876(49)	0.4857(50)	0.4791(50)
eQq(Br)	223.874(61)	223.858(45)	187.013(45)	187.028(45)
	$^{18}O^{12}C^{107}Ag^{79}Br$	$^{18}O^{12}C^{109}Ag^{79}Br$	$^{18}O^{12}C^{107}Ag^{81}Br$	$^{18}O^{12}C^{109}Ag^{81}Br$
B_0	814.879783(49)	814.254632(49)	805.795502(52)	805.140418(49)
$D_J \times 10^4$	0.4451(35)	0.4494(35)	0.4346(36)	0.4372(35)
eQq(Br)	223.827(59)	223.965(60)	187.128(63)	186.937(60)

[a] Numbers in parentheses are 1 SD in units of the last significant figure.

Table 4. Experimental and ab Initio Bond Lengths for OCAgX in Ångstroms

method	r(CO)	r(CAg)	r(AgX)
	OCAgF		
r_0	1.12553(5)[a]	1.96501(7)	1.94382(7)
$r_{I\epsilon}$	1.125550(5)	1.96528(2)	1.9419(1)
$r_m^{(1)}$	1.125310(2)	1.96486(1)	1.9415(2)
MP2[b]	1.138	1.907	1.932
	OCAgCl		
r_0	1.122(1)	2.016(1)	2.2548(6)
$r_{I\epsilon}$	1.12446(9)	2.0125(1)	2.25289(5)
$r_m^{(1)}$	1.12369(8)	2.0111(1)	2.25134(8)
$r_m^{(2)}$	1.1215(1)	2.01281(9)	2.25036(5)
MP2[b]	1.137	1.965	2.267
MP2[c]	1.137	1.947	2.254
B3LYP[d]	1.124	2.097	2.338
	OCAgBr		
r_0	1.1236(9)	2.027(1)	2.3731(5)
$r_{I\epsilon}$	1.1242(1)	2.0275(1)	2.3704(2)
$r_m^{(1)}$	1.1236(1)	2.0264(2)	2.3692(2)
$r_m^{(2)}$	1.1219(4)	2.02800(4)	2.36826(2)
MP2[b]	1.137	1.979	2.344

[a] Numbers in parentheses are 1 SD in units of the last significant figure. [b] This work. [c] Ref 13. [d] Ref 15.

an $r_{I\epsilon}$ structure, the bond lengths are typically better determined than the corresponding r_0 distances.

***Mass-Dependent Geometries* − $r_m^{(1)}$, $r_m^{(2)}$.** The mass dependence of the contribution made by vibrational effects to the rotational constant of a given molecule is acknowledged through the calculation of a mass-dependent (r_m) geometry,[37] following the equation

$$I_0 = I_m(r_m) + c(I_m(r_m))^{1/2} + d((m_1m_2m_3m_4)/M)^{1/6} \quad (6)$$

where M is the sum of the atomic masses m_i of a given isotopomer, c and d are constants, and $I_m(r_m)$ is the moment of inertia using the rigid rotor expression with the resulting internuclear distances. Where d is set to zero, this calculation permits c and the $r_m^{(1)}$ bond distances to be determined through fitting to the experimental moments of inertia. If both c and d are included in the fits, then an $r_m^{(2)}$ geometry is determined. The $r_m^{(2)}$ structure provides probably the closest approximation to the r_e structure that can be obtained from ground vibrational state data alone. The r_m distances calculated are shown alongside the results obtained from the other methods in Table 4. In general, there is good agreement between the results obtained from the different calculation methods.

B. Ab Initio Structural Parameters. The results from structural fits are compared with those from theoretical calculations in Table 4. Theoretical data are available from the work of Antes et al.[13] and Shao et al.[15] for OCAgCl, and

(37) Watson, J. K. G.; Roytburg, A.; Ulrich, W. *J. Mol. Spectrosc.* **1999**, *196*, 102.

Table 5. Experimental and ab Initio Bond Lengths (Å) of AgX

	MP2[a]	r/Å
AgF	1.977	1.983[b]
AgCl	2.289	2.281[c]
AgBr	2.370	2.393[d]

[a] This work. [b] Ref 40. [c] Ref 41. [d] Ref 42.

calculations performed during this work permit comparison of experimental and theoretical data for OCAgF and OCAgBr. The calculations performed herein were conducted at the same level of theory as was employed by Antes et al.,[13] and the results obtained for OCAgCl are consequently very similar. Corresponding calculations were also performed on the diatomic metal halides, AgF, AgCl, and AgBr; these results are displayed in Table 5, where it can be seen that there is good agreement with experimental results.

For the complexes, the theoretical geometries differ significantly from the experimental results. For example, while the density functional (B3LYP) calculation gives a good prediction of r(CO), the MP2 values are consistently more than 0.01 Å too high. It is interesting that MP2 calculation also produces the same discrepancy for free CO.

The MP2 calculation does comparatively well with the Ag−X distances. The calculated values are somewhat too low for the fluoride and bromide and somewhat high for the chloride; these variations parallel those obtained for the AgX monomers. The B3LYP values for r(AgCl) are really quite poor: ∼0.09 Å too large. Finally, neither method does well for r(AgC). The MP2 values are low by 0.04−0.06 Å; the B3LYP value for OCAgCl is 0.08 Å too high.

VI. Vibrational Frequencies

The distortion constant (D_J) provides an indication of the rigidity of a molecule and is intimately related to its vibrational frequencies. A pseudodiatomic approximation can be used to predict the vibrational stretch of lowest frequency for each molecule, using eq 7. (It should be noted that significant contributions to the measured value of D_J could be expected from both the Ag−C and Ag−X bonds, so the calculated vibrational frequencies are not necessarily determined to a high level of accuracy.)

$$\omega \approx \left(\frac{4B_0^3}{D_J}\right)^{1/2} \tag{7}$$

Applying this expression to the data obtained from OCAgF, OCAgCl, and OCAgBr yields values of 355, 299, and 235 cm^{-1}, respectively. These results are presented in Table 6 alongside the results of MP2 calculations on the various molecules studied. Calculations were also performed for monomeric AgF, AgCl, and CO; these results are presented in Table 7 and show calculated values which are in good agreement with experimental measurements.

The vibrational stretch of lowest frequency is the M−C stretch in the case of the OCAgF but is the M−X stretch for OCAgCl. The result obtained from the experimentally measured distortion constant is 35 cm^{-1} lower than the MP2 result in the case of the fluoride. The agreement is better for the chloride. The value of 299 cm^{-1} obtained from the distortion constant is within 12 cm^{-1} of the MP2 result obtained during this work, and within 30 cm^{-1} of that obtained by Antes et al.[13]

The vibrational wavenumbers were calculated for OCAgBr using the same method and basis sets as were used for the geometry and Mulliken orbital population calculations. However, imaginary frequencies were predicted for several modes, and therefore, data are not presented here.

Table 6. Experimental and ab Initio Vibrational Wavenumbers of OCAgX (cm^{-1})

	method	Σ CO str[b]	Σ MC str	Π MCO def	Σ MX str	Π XMC def	expt[c]
OCAgF	MP2[a]	2146.5	390.9	347.2	589.7	88.4	355
OCAgCl	MP2[a]	2147.2[d]	397.5	314.5	310.8	63.7	299
	MP2[e]	2145.5[d]	413.5	328.1	324.7	67.9	
	B3LYP[f]	2235[d]	341	273	244	57	

[a] This work. [b] Experimentally measured value for free CO is 2138 cm^{-1} (ref 43). [c] From the experimentally measured distortion constants. The result for OCAgBr was 235 cm^{-1}. [d] Experimental value: 2184.0 cm^{-1} (ref 15). [e] Ref 13. [f] Ref 15.

Table 7. Experimental and ab Initio Vibrational Wavenumbers of AgX (cm^{-1})

	MP2[a]	expt
AgF	529.4	513.0[b]
AgCl	338.0	343.5[c]
CO	2134.1	2138[d]

[a] This work. [b] Barrow, R. F.; Clements, R. M. *Proc. R. Soc. London, Ser. A.* **1971**, *322*, 243. [c] Brice, B. *Phys. Rev.* **1931**, *22*, 573. [d] Ref 43.

Table 8. Nuclear Quadrupole Coupling Constants of M, Cl, and Br in Various OCMX Species in Megahertz

	OCMX[a]		ArMX		MX	
MX[a]	eQq(M)[a]	eQq(X)	eQq(M)	eQq(X)	eQq(M)	eQq(X)
CuF	75.406[b]		38.055[c]		21.956[c]	
CuCl	70.832[b]	−21.474[b]	33.186[c]	−28.032[c]	16.169[d]	−32.127[d]
CuBr	67.534[b]	171.600[b]	29.923[c]	225.554[c]	12.851[d]	261.180[d]
AgCl		−28.151[e]		−34.486[f]		−36.440[g]
AgBr		223.902[e]		278.888[f]		297.047[h]
AuF	−1006.3[i]		−333.4[j]		−53.31[k]	
AuCl	−1026.0[i]	−36.39[i]	−259.8[l]	−54.05[l]	9.633[m]	−61.99[m]
AuBr	−999.1[i]	285.09[i]	−216.7[j]	428.5[j]	37.26[m]	492.3[m]

[a] Data are for ^{19}F, ^{35}Cl and ^{79}Br isotopes, respectively. [b] Ref 14. [c] Ref 17. [d] Low, R. J.; Varberg, T. D.; Connelly, J. P.; Auty, A. P.; Howard, B. J.; Brown, J. M. *J. Mol. Spectrosc.* **1993**, *161*, 499. [e] This work. [f] Ref 16. [g] Ref 41. [h] Ref 42. [i] Ref 4. [j] Ref 19. [k] Evans, C. J.; Gerry, M. C. L. *J. Am. Chem. Soc.* **2000**, *122*, 1560. [l] Ref 18. [m] Evans, C. J.; Gerry, M. C. L. *J. Mol. Spectrosc.* **2000**, *203*, 105.

VII. Nuclear Quadrupole Coupling Constants

Nuclear quadrupole coupling constants were determined for the halogen atoms in OCAgCl and OCAgBr and are shown in Table 8. This quantity provides an indication of the degree of charge rearrangement with respect to the analogous metal halide. When the carbonyl is formed, there are substantial changes in the eQq(X) of both the chlorine and bromine atoms upon the attachment of CO to the silver halide. The changes in eQq(X) with the attachment of argon to AgCl and AgBr are also shown in Table 8. As might be expected, the degree of charge rearrangement associated with the attachment of the noble gas is not as great as that observed on the addition of CO to AgX.

Table 9. MP2 Mulliken Orbital Populations for OCAgX

	FAgCO	AgF + CO	ClAgCO	AgCl + CO	BrAgCO	AgBr + CO
q^X	−0.65	−0.68	−0.63	−0.67	−0.84	−0.84
n_s^X	2.00	2.00	2.00	2.00	2.00	2.00
$n_{p\sigma}^X$	1.80	1.82	1.75	1.77	1.81	1.83
$n_{p\pi}^X$	3.85	3.87	3.96	4.00	3.91	3.95
$n_{d\sigma}^X$					2.00	2.00
$n_{d\pi}^X$					4.00	4.00
$n_{d\delta}^X$					4.00	4.00
q^{Ag}	0.63	0.68	0.64	0.67	0.81	0.84
n_s^{Ag}	0.44	0.19	0.50	0.24	0.37	0.16
$n_{p\sigma}^{Ag}$	0.01	0.03	0.00	0.04	0.00	0.00
$n_{p\pi}^{Ag}$	0.07	0.07	0.07	0.07	0.10	0.05
$n_{d\sigma}^{Ag}$	1.84	1.96	1.88	1.97	1.85	1.96
$n_{d\pi}^{Ag}$	3.94	4.00	3.93	4.00	3.91	4.00
$n_{d\delta}^{Ag}$	4.00	4.00	4.00	4.00	4.00	4.00
q^C	0.19	0.21	0.15	0.21	0.21	0.21
n_s^C	1.62	1.77	1.65	1.77	1.69	1.77
$n_{p\sigma}^C$	0.97	0.97	0.99	0.97	0.97	0.97
$n_{p\pi}^C$	1.10	0.94	1.09	0.94	1.02	0.94
$n_{d\sigma}^C$	0.03	0.03	0.03	0.03	0.03	0.03
$n_{d\pi}^C$	0.10	0.08	0.09	0.08	0.08	0.08
q^O	−0.17	−0.21	−0.17	−0.21	−0.18	−0.21
n_s^O	1.88	1.82	1.88	1.82	1.88	1.82
$n_{p\sigma}^O$	1.38	1.40	1.37	1.40	1.38	1.40
$n_{p\pi}^O$	2.90	2.96	2.90	2.96	2.90	2.96

Antes et al.[13] calculated the Cl electric field gradients of AgCl and OCAgCl to be −1.657 and −1.386 au (−1.610 × 10^{22} and −1.347 × 10^{22} V m^{-2}), respectively. Nuclear quadrupole coupling constants were calculated from these electric field gradients by assuming a value of −8.249 fm^2 for the nuclear quadrupole moment of ^{35}Cl. Values of −32.1 and −26.9 MHz are obtained, in moderate agreement with the experimentally determined quantities of −36.4408 and −28.15045 MHz.

The results of Mulliken valence orbital population analyses are shown in Table 9. On the attachment of CO to AgF, there are decreases in the $n_{d\sigma}^{Ag}$ and $n_{d\pi}^{Ag}$ orbital populations of 0.12 and 0.06, respectively. There is a significant decrease (0.15) in the n_s^C population and also a smaller decrease in the $n_{p\pi}^O$ population (0.06). This is accompanied by substantial increases of 0.25 and 0.16 in the n_s^{Ag} and $n_{p\pi}^C$ orbital populations, respectively, and an increase of 0.06 in the n_s^O population.

Changes in the orbital populations on formation of OCAgCl and OCAgBr follow similar trends to those described above for OCAgF and are of comparable magnitude. The general trend for OCAgCl is in agreement with the analysis presented earlier by Antes et al. An electron density contour plot of OCAgCl (prepared using MOLDEN 3.4[38]) is provided in Figure 5.

The well-known Townes−Dailey[34] model of quadrupole coupling can be applied, incorporating the Mulliken populations. It is only partially successful. In this model, the coupling constants are given by

$$eQq = eQq_{n10}\left(n_\sigma - \frac{n_\pi}{2}\right) \quad (8)$$

where eQq_{n10} is the coupling constant for a singly occupied 3p orbital on Cl (=109.74 MHz for ^{35}Cl) and for a singly occupied 4p orbital on Br (=−769.76 MHz for ^{79}Br). When the values of n_σ and n_π for the monomers from Table 9 are inserted, the values obtained for eQq are −25.2 MHz for Ag^{35}Cl and 111.6 MHz for Ag^{79}Br.[34] The result for the chloride is in moderate agreement with experiment, but that for the bromide is significantly different from the measured quantity. The model also predicts no change on complex formation, in strong contrast with experiment. Clearly, the model is oversimplified in this case.

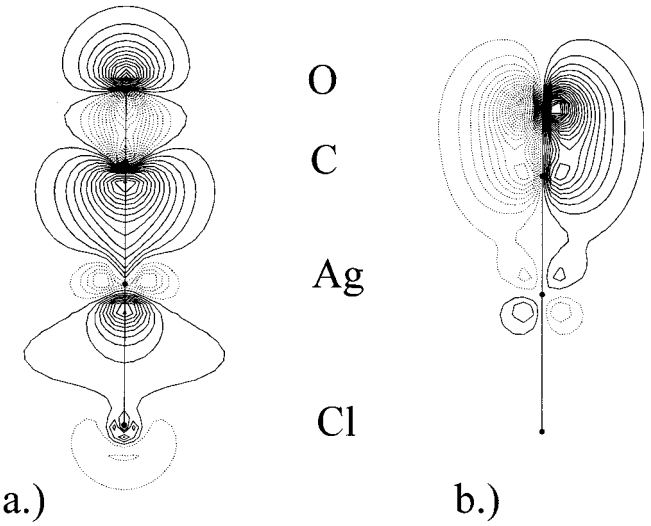

Figure 5. Contour diagrams of electron density of the (a) 10σ and (b) 3π molecular orbitals of OCAgCl. The dotted and solid lines indicate different signs of the molecular orbital wave functions.

VIII. Discussion and Conclusions

The microwave spectra of the carbonyl halides OCMX (X = F, Cl, Br) have now been reported for all three coinage metals, M = Cu, Ag, Au. Of the Ag complexes, only OCAgCl has been mentioned previously in the literature; experimental evidence for it was scarce,[15] and it was thought to be difficult to prepare.[13] However, it was straightforward to generate in the present experiments, as were OCAgF and OCAgBr. For the fluoride and bromide, this is the first report of any kind, theoretical or experimental. Laser ablation is clearly an ideal method for generating these molecules provided they are subsequently stabilized within the collision-free environment provided by a supersonic jet. The Ag complexes were no more difficult to prepare and study by this method than the apparently more stable[13] Cu and Au complexes,[4,14] several of which were already well characterized.[7−12] The present work has characterized the Ag complexes thoroughly and has provided a large amount of structural information.

The internuclear distances determined in this work are presented in comparison with those of several related metal

(38) Schaftenaar, G. *MOLDEN 3.4*; CAOS/CAMM Center: The Netherlands, 1998.

Table 10. Bond Lengths of Various Metal Carbonyl Species in Ångstroms

	M−C	C−O	comments
OCCuF	1.765	1.131	$r_{l\epsilon}$ values,[a] (FTMW, ref 14)
OCCuCl	1.795	1.129	$r_{l\epsilon}$ values, (FTMW, ref 14)
OCCuBr	1.803	1.128	$r_{l\epsilon}$ values, (FTMW, ref 14)
OCAgF	1.965	1.126	$r_{l\epsilon}$ values, this work
OCAgCl	2.013	1.124	$r_{l\epsilon}$ values, this work
OCAgBr	2.028	1.124	$r_{l\epsilon}$ values, this work
OCAuF	1.847	1.134	r_0 values (FTMW, ref 4)
OCAuCl	1.883	1.132	$r_{l\epsilon}$ values (FTMW, ref 4)
OCAuBr	1.892	1.132	$r_{l\epsilon}$ values (FTMW, ref 4)
PtCO	1.760	1.148	$r_{l\epsilon}$ values, ref 44
NiCO	1.687	1.166	CCSD, ref 45
FeCO	1.727	1.160	$r_{l\epsilon}$ value, ref 46
$Ni(CO)_4$	1.838	1.141	electron diffraction, ref 47
$Fe(CO)_5$	1.833	1.145	electron diffraction, ref 48
CO		1.128	r_e value, ref 43

[a] The $r_{l\epsilon}$ values are given in order to allow comparison with the bond lengths of OC−AuX. The preferred r_m values (Table 4) are up to 0.001 Å shorter.

carbonyls in Table 10. As with the Cu and Au complexes, the C−O bonds are short, comparable to that in free CO, and are very much shorter than those of the other molecules. Indeed, the C−O bonds of the Ag complexes are apparently significantly shorter than those of the other coinage metal complexes, and even that of CO itself. The CO stretching frequencies measured experimentally are 2138 cm^{-1} for free CO, and 2156, 2184, and 2162 cm^{-1} for OCMCl where M = Cu, Ag, and Au, respectively.[8,12,15] There is a reasonable correlation between the C−O bond distances and measured CO stretching frequencies of the various chlorides; OCAgCl has both the shortest bond and the highest stretching frequency. However, all the stretching frequencies are greater than that of free CO itself, so the corresponding correlation does not apply in this case. The Ag−C bonds are all significantly longer than the Cu−C and Au−C bonds in the corresponding complexes. This trend was predicted by Antes et al.[13] for the chlorides and is the result of relativistic contributions to the electronic structures of Au and its compounds. It may be noted that the Au−C bond in OCAuX is longer than the Pt−C bond in PtCO. It can thus be surmised that the Pd−C bond in the palladium derivative, PdCO, should be longer than the Pt−C bond in PtCO but shorter than the Ag−C bond in OCAgX. Recent experiments on PdCO[39] have shown this to be the case; these results will be published shortly.

It is clear also from the comparisons in Table 10 that for all the OCMX molecules the bonding for the fluorides is different from that of the corresponding chlorides and bromides. The M−C bonds are shorter in the fluorides by 0.03−0.05 Å; the C−O bonds are longer by about 0.002 Å. For the Au and Cu derivatives, the metal quadrupole coupling constants of the fluorides do not conform to the systematic trends set by the chlorides and bromides,[4,14] in contrast to the ArMX complexes.[16−21] It is difficult to explain these differences. However, ab initio calculations for OCAuF and OCAuCl seemed to show greater electron density in the AuF parts of the bonding molecular orbitals than in the AuCl parts. A similar phenomenon probably applies throughout.

Another interesting phenomenon is the fractional change of the halogen quadrupole coupling constants on complex formation (i.e., the ratio of the halogen coupling constant of the complex to that of the monomer). These are ∼0.66, ∼0.77, and ∼0.59 for the Cu, Ag, and Au complexes, respectively. The implication in this case is that electron rearrangement is the least in the formation of the Ag complexes, consistent with their greater M−C internuclear distances.

The calculated Mulliken populations agree mildly with the structures. The largest σ-donation from, and π-donation to, C is found for the fluoride, and the smallest is found for the bromide. In all cases, some degree of π-back-bonding is found, which in a simple picture of the bonding would imply a lengthening of the C−O bond and a decrease of the stretching frequency; both are contrary to experiment. Antes et al.[13] suggested that the increase in the stretching frequency is due to electrostatic factors. It is likely that variation in these parameters results from a subtle combination of several effects, including, for example, the degrees of σ- and π-donation and the relative charges at the various atoms in the molecule. Overall, the structural properties of the OCMX complexes have been found to be much as expected. The short C−O bonds and relatively long M−C bonds follow the trends predicted earlier, at least qualitatively. Predicted relativistic effects are clear. However, thus far, ab initio predictions have been somewhat less than quantitative, in general. The experimental results will provide benchmarks for future calculations.

Acknowledgment. The research has been supported by the Natural Sciences and Engineering Research Council (NSERC) of Canada and by the Petroleum Research Fund, administered by the American Chemical Society.

Supporting Information Available: Measured rotational transition frequencies of OCAgX (X = F, Cl, Br). This material is available free of charge via the Internet at http://pubs.acs.org.

IC010997M

(39) Walker, N. R.; Hui, J. K. H.; Gerry, M. C. L. *J. Phys. Chem.*, submitted.
(40) Hoeft, J.; Lovas, F. J.; Tiemann, E.; Törring, T. *Z. Naturforsch., A: Phys. Sci.* **1970**, *25*, 35.
(41) Hensel, K. D.; Styger, C.; Jäger, W.; Merer, A. J.; Gerry, M. C. L. *J. Chem. Phys*. **1993**, *99*, 3320.
(42) Hoeft, J.; Lovas, F. J.; Tiemann, E.; Törring, T. *Z. Naturforsch., A: Phys. Sci.* **1971**, *26*, 240.
(43) Huber, K. P.; Herzberg, G. *Molecular Spectra and Molecular Structure: Constants of Diatomic Molecules*; Van Nostrand: New York, 1979.
(44) Evans, C. J.; Gerry, M. C. L. *J. Phys. Chem. A.* **2001**, *105*, 9659.
(45) Solupe, M.; Bauschlicher, C. W., Jr.; Lee, T. J. *Chem. Phys. Lett.* **1992**, *189*, 266.
(46) Kasai, Y.; Obi, K.; Ohshima, Y.; Endo, Y.; Kawaguchi, K. *J. Chem. Phys*. **1995**, *103*, 90.
(47) Hedberg, L.; Iijuma, T.; Hedberg, K. *J. Chem. Phys.* **1958**, *70*, 3224.
(48) Beagley, B.; Cruickshank, D. W. J.; Pinder, P. M.; Robiette, A. G.; Sheldrick, G. M. *Acta Crystallogr*. **1969**, *B25*, 737.